Atmos. Chem. Phys. Discuss., 5, 6041–6076, 2005
www.atmos-chem-phys.org/acpd/5/6041/
SRef-ID: 1680-7375/acpd/2005-5-6041
European Geosciences Union

Atmospheric Chemistry and Physics Discussions

Atmospheric oxidation in the Mexico City Metropolitan Area (MCMA) during April 2003

T. R. Shirley[1], W. H. Brune[1], X. Ren[1], J. Mao[1], R. Lesher[1], B. Cardenas[2], R. Volkamer[3], L. T. Molina[3], M. J. Molina[3], B. Lamb[4], E. Velasco[4], T. Jobson[5], and M. Alexander[5]

[1]Dept. of Meteorology, Pennsylvania State University, University Park, Pennsylvania, USA
[2]General Direction of the National Center for Environmental Research and Training (CENICA), National Institute of Ecology (INE), Mexico City, Mexico
[3]Dept. of Earth, Atmospheric, and Planetary Sciences, Massachusetts Institute of Technology, Cambridge, Massachusetts, USA
[4]Dept. of Civil and Environmental Engineering, Washington State University, Pullman, Washington, USA
[5]Atmospheric Sciences, Pacific Northwest National Laboratory, Richland, Washington, USA

Received: 1 July 2005 – Accepted: 15 July 2005 – Published: 17 August 2005

Correspondence to: W. H. Brune (brune@ems.psu.edu)

Abstract

The Mexico City Metropolitan Area (MCMA) study in April 2003 had measurements of most atmospheric constituents including OH and HO_2. It provided a unique opportunity to examine atmospheric oxidation in a megacity that has more pollution than typical US and European cities. OH typically reached 0.35 pptv (~7×10^6 cm^{-3}), comparable to amounts observed in US cities, but HO_2 reached 40 pptv in the early afternoon, more than observed in most US cities. A steady-state photochemical model simulated the measured OH and HO_2 for day and night to within combined measurement and modeling uncertainties for 2/3 of the results. For OH, measured = 0.65 (modeled) + 0.026 pptv, with R^2=0.80. For HO_2, observed = 0.70 (modeled) + 3.4 pptv, with R^2=0.64. Measurements tended to be higher during night and rush hour; the model was higher by ~30% during midday. With a large median measured OH reactivity of more than 120 s^{-1} during morning rush hour, median ozone production from observed HO_2 reached 50 ppb hr^{-1}; RO_2 was calculated to have a similar ozone production rate. For both the HO_2/OH ratio and the ozone production, the measured values have the essentially same dependence on NO as the modeled values. This similarity is unlike other urban studies in which the NO-dependence of the measured HO_2/OH ratio was much less than the modeled ratio and the ozone production rate that was calculated from measured HO_2 unexpectedly appeared to increase as a function of NO with no obvious peak.

1. Introduction

Megacities contain not only millions of people but also elevated levels of airborne pollutants. These pollutants are generated by the transportation and industry necessary to support these millions. The fast chemistry that transforms primary pollutant emissions of nitrogen oxides (NO_x) and volatile organic compounds (VOCs) is initiated by reactions of the hydroxyl radical, OH, with VOCs. The subsequent reactions produce

ACPD

5, 6041–6076, 2005

the hydroperoxyl radical, HO_2, which reacts with NO to reform OH and create NO_2, resulting in the production of the pollutant ozone (O_3). Low volatility VOCs are also generated, resulting in the formation of secondary organic aerosol mass. Together, OH and HO_2, called HO_x, form a rapid reaction cycle that drives this atmospheric chemistry.

Several field studies that include HO_x measurements have been conducted in urban environments in the United States, including Los Angeles, California (George et al., 1999), Nashville, Tennessee (Martinez et al., 2003), Houston, Texas (Martinez et al., 2002) and New York City, New York (Ren et al., 2003a). Field studies with HO_x measurements have also been conducted in urban air in Europe as well, including Berlin, Germany (Volz-Thomas et al., 2003, and accompanying papers) and Birmingham, United Kingdom (Heard et al., 2004; Emmerson et al., 2005). The Mexico City Metropolitan Area (MCMA), a megacity, has more pollution than any of these other urban environments (Molina and Molina, 2002).

OH and HO_2 and other atmospheric constituents important for studying atmospheric oxidation were measured during the Mexico City Metropolitan Area 2003 (MCMA-2003) study, which was held in the MCMA during April 2003. MCMA is at a high altitude (~2240 m) near the equator at 19°25′ N latitude. At this high altitude and low latitude, intense solar radiation penetrates to the surface causing active photochemistry. In addition to the radiation, the area's orography, with mountains to the west, east, and south of the metropolitan area, traps pollutants in the basin. As a result, MCMA experiences high pollution levels. These simultaneous measurements were an opportunity to develop a better understanding of MCMA's high pollution levels of ozone and secondary particulate matter. They also stretch the envelope of polluted environments that have been studied with a complete measurement suite that includes measurements of the radicals OH and HO_2.

2. Description of the MCMA 2003 study

2.1. Site description

Measurements of OH and HO_2 were made from the roof of the building that houses the National Center of Investigation and Environmental Qualification (CENICA) on the Iztapalapa campus of the Autonomous Metropolitan University in Iztapalapa, Mexico City. Iztapalapa lies in the south-central MCMA, due south of the downtown area by ~7 km. The university is located in a semi-residential and semi-industrial area. To the west and south of the university are mainly residential areas; to the north and east are several factories and industries.

Northerly (southward) wind, which is usually the dominant surface-wind direction during the daytime hours, generally brings air from the downtown to this site. The winds from all other directions bring air from the surrounding suburbs to the site. In contrast to mid-latitude megacities, high pollution episodes can occur year-round in the MCMA because the subtropical highs that dominate the weather throughout the year are conducive to active photochemistry. During the winter and spring months, the area is normally under an anticyclone with light winds and clear skies. As a result, strong surface-based inversions usually persisted several hours into the morning. Strong solar heating eventually breaks down the inversion and pollutants then mix into a very deep boundary layer of around four km. This study was held in April to avoid the wetter summer months (June–September) because clouds and precipitation inhibit strong photochemistry (Molina and Molina, 2002). However, in 2003, the summertime pattern began in April, resulting in frequent clouds and some rain in the afternoon.

2.2. GTHOS (Ground-based Tropospheric Hydrogen Oxides Sensor)

OH and HO_2 were measured by the Penn State Ground-based Hydrogen Oxides Sensor, called GTHOS. A brief description of the measurement technique and instrument is given here; a full description can be found in Faloona et al. (2004). GTHOS mea-

ACPD
5, 6041–6076, 2005

surement of OH and HO_2 is based on FAGE (Fluorescence Assay by Gas Expansion) (Hard et al., 1984). The air sample is drawn through an orifice (1.0 mm diameter) into a low-pressure chamber at a pressure of 4–5 hPa. As the air passes through a laser beam, OH is excited by the laser and then detected at a wavelength near 308 nm. Collisional quenching of the excited state is slow enough at the chamber pressure that the weak OH fluorescence extends beyond the prompt scattering (Rayleigh and wall scattering) and is detected with a time-gated microchannel plate (MCP) detector.

OH is detected in the first of two detection axes. In a second axis, HO_2 is chemically converted to OH by reaction with reagent NO that is added to the flow between the two axes. The resultant OH is then detected by LIF. The laser wavelength is turned on and off resonance with an OH transition every 10 s. The OH fluorescence signal is the difference between on-resonance and off-resonance signals.

GTHOS was calibrated before, during, and after the study using the techniques described in Faloona et al. (2004). The upper-limit of the absolute calibration uncertainty was estimated at ±32% (at the 95% – 2 σ-confidence level). The OH detection limit can be defined from twice the standard deviation of the background signal and was 0.01 part per trillion by volume, or pptv, ($\sim 2\times10^5$ cm^{-3}) for a 1-min integration period. The HO_2 detection limit (with 2σ-confidence, 1-min integration time) was estimated to be 0.1 pptv ($\sim 2.0\times10^6$ cm^{-3}).

During the campaign in Mexico City, GTHOS was mounted approximately 18 m above the ground on the third level of a scaffolding tower (Fig. 1). Ambient air was pulled through the system by a vacuum pump that was located directly beneath the measurement tower. The electronics and calibration equipment were housed in an air-conditioned hut that was directly adjacent to the tower.

2.3. TOHLM (Total OH Loss Measurement)

The first-order OH loss rate, called the OH reactivity, was measured with the Total OH Loss Measurement instrument (TOHLM) (Kovacs and Brune, 2001; Kovacs et al., 2003; DiCarlo et al., 2004). It was mounted on the first level of the tower, approximately

14 m above the ground. The inlet hose for TOHLM was mounted just below the inlet of GTHOS on the third level of the tower.

The TOHLM method is analogous to the discharge-flow technique used in laboratory kinetics studies. OH is generated at mixing ratios of a few 10's of parts per trillion by volume (pptv) by ultraviolet light from a mercury lamp. This light photodissociates water vapor, creating OH and H in a nitrogen flow inside a 1-cm diameter movable tube. H rapidly reacts with trace O_2 in the N_2 to form HO_2. This moveable tube is in the center of a 7.5-cm diameter glass flow tube through which ambient air is drawn by a fan with a total sampling flow rate of about 140 l min^{-1} and a residence time of 0.1–0.4 s. The OH is injected through radially drilled holes at the end of the movable tube, mixed turbulently into the air flow, and detected by an OH detector at the end of the flow tube. The detection technique is low-pressure laser induced fluorescence, as is used for GTHOS. OH reacts with trace constituents in the air flow and, as the movable tube is drawn further away from the detector, the observed OH signal decreases.

The OH reactivity, k_{OH}, is the slope of the logarithm of the OH signal, S^{OH}, as function of the time (the distance divided by the velocity) minus the OH loss to the flow tube's walls, k_{wall}:

$$k_{OH} = -\Delta \ln\left(S^{OH}\right) / \Delta\text{time} - k_{wall} \quad (1)$$

Each decay took 4.3 min, with 20 s at each of 13 steps, 10 s measuring OH plus the background signal and 10 s measuring the background signal. The OH signal decreased by a factor of 10–20 over the 13 steps. Typically, the OH wall loss rate, k_{wall}, was $1.5 \pm 0.4\ s^{-1}$. Generally, OH mixing ratios were 10–30 pptv inside the glass tubing.

2.4. TOHLM correction technique

Kovacs et al. (2003) and Ren et al. (2003a) discuss the need to correct OH reactivity measurements for the OH-recycling reaction:

$$HO_2 + NO \rightarrow OH + NO_2 \quad (R1)$$

ACPD
5, 6041–6076, 2005

When levels of NO are below 1 ppbv, the measured decays are generally linear and the slopes correct to within 10% (Kovacs et al., 2003). However, when ambient levels of NO are higher, the decays have concave curvature as HO_2 reacts with the NO to reform OH. In past studies where the TOHLM instrument was used, NO concentrations infrequently reached levels that required significant corrections or measurements from those times were excluded from further analysis. However, in MCMA during rush hour (05:00–09:00 CST), NO exceeded 50 ppbv 40% of the time and 100 ppbv 12% of the time. This frequent contamination of the decays led to a need for a new correction technique that allows k_{OH} to be measured at much higher values of NO than earlier methods (Kovacs et al., 2003).

The rate equation for [OH] is given by the expression:

$$\begin{aligned}\frac{d[OH]}{dt} &= -k_{OH}[OH] + k_{NO+HO2}[NO][HO_2] \\ &= -k_{OH}[OH] + k_{NO+HO2}[NO]R[OH]\end{aligned} \quad (2)$$

where k_{OH} is the OH reactivity (s^{-1}) and R is the measured $[HO_2]/[OH]$ ratio. Assuming that the average value for R can be used for each time step, this expression can be integrated to give the value of [OH] at time step t_1:

$$[OH]_1 = [OH]_0 \exp(-k_{OH}(t_1 - t_0)) \exp(+k_{NO+HO2}[NO]\,R\,(t_1 - t_0)) \quad (3)$$

The desired [OH] value is given by the expression $[OH]_0 \exp(-k_{OH}\,(t_1 - t_0))$. Thus the corrected [OH] at time t_1 is given by the expression:

$$[OH]_1^c = [OH]_1 \exp\left(-\frac{k_{NO+HO2}[NO]\,[HO_2]_{0,1}\,(t_1 - t_0)}{[OH]_{0,1}}\right) \quad (4)$$

where $[OH]_{0,1}$ and $[HO_2]_{0,1}$ are average concentrations of times 0 and 1. Since the observed OH and HO_2 signals are proportional to [OH] and $[HO_2]$ by the calibration factors, C_{OH} and C_{HO2}, which for TOHLM are the same, the OH signal can be corrected for the first time step by the expression:

$$S_1^c = \exp[-(\Delta S_1 / S_{0,1})] * S_1 \quad (5)$$

where $\Delta S_1 = k_{NO+HO2}$ [NO] $S^{HO2}_{0,1}$ $(t_1 - t_0)$ and $S^{HO2}_{0,1}$ is the averaged HO_2 signal for times t_0 and t_1.

In order to correct subsequent points, we must realize that the points are not independent of one another. Points S_1 and S_2 are then scaled by S^c_1 by multiplying by S^c_1/S_1, so that the slope between S_1 and S_2 is preserved but the starting point is S^c_1 (Fig. 2). The correction given in Eq. (4) is then applied to S_2 and the equation for S^c_2 takes the form:

$$S^c_2 = \exp[-(\Delta S_1/S_{0,1})] * \exp[-(\Delta S_2/S_{1,2})] * S_2 \quad (6)$$

where $\exp[-(\Delta S_1/S_{0,1})]$ is simply the S^c_1/S_1 that was calculated in Eq. (5). Each subsequent point is calculated in this manner assuring that each point is scaled to the one before it.

This correction technique was tested in the laboratory (Fig. 3). In this example, NO was ~75 ppbv, a normal rush-hour value for Mexico City. The theoretical calculated decay from the NO and ultra zero air mixture is 14.9 s^{-1}. The uncorrected decay, 8.87 s^{-1}, is only 60% of what is calculated, while the corrected decay is 14.6 s^{-1}. Agreement between the calculated and corrected decays is well within the uncertainties of the TOHLM technique and the reaction rate coefficient for OH + NO + M → HONO + M.

This correction technique was used on a wide range of NO concentrations, from 10–200 ppbv (Fig. 4). To ensure that this technique would work when other reactants were present, several different concentrations of CO were added to the instrument along with the NO. In all but one case (with and without the addition of CO) the corrected OH decays were within 15% of the theoretical values. However, the correction factor for decays when NO>100 ppbv grows to a factor of ~2–3 and becomes more uncertain, since small errors in S^{HO2}/S^{OH} ratio and in NO become more important. Using estimates of the uncertainties in these two terms and considering the number of points used in the decays, we estimate that the uncertainty in the correction is ~10%, 1σ confidence. Because the correction for 75 pptv of NO is roughly 1.7, the total absolute uncertainty for the corrected OH reactivity is ±25%, 1σ confidence, for 75 pptb of NO.

2.5. Model description

OH and HO_2 measurements were compared to a constrained steady-state photochemical model, which is briefly described here. A more complete description can be found in Ren et al. (2003b). During the MCMA campaign the following ancillary data were continuously measured: O_3, CO, SO_2, NO, NO_2, CH_4, HCHO, HONO, temperature, pressure, relative humidity, wind speed, and wind direction. Speciated VOCs were measured at CENICA for four days before and three days after the HO_x measurements (Lamb et al., 2004) and were measured at other locations while HO_x was being measured at CENICA. These speciated VOCs were averaged for each half-hour that they were measured over the seven days and summed into VOC types (e.g., internal alkenes) that the model uses. For the model calculations, the abundance for each VOC type was determined by assigning the same fraction of the measured OH reactivity from VOCs to that VOC type and then calculating the VOC type's abundance from that fraction of the OH reactivity divided by the reaction rate coefficient. Since the standard deviation of each fraction was generally less than 35% and the fraction of OH reactivity due to each VOC type was similar at CENICA and three other urban sites, this method should work in an average sense. This method has been shown to give good results between measured and modeled HO_x in other studies (Ren et al., 2005a, b[1]).

The Regional Atmospheric Chemistry Mechanism (RACM) (Stockwell et al., 1997) was used to calculate the OH and HO_2 concentrations. Kinetic rate coefficients were updated using the results by Sander et al. (2003). Reactions of O_3 with alkenes have been largely revised to represent latest radical yields suggested by recent experiments (Paulson et al., 1999; Rickard et al., 1999; Fenske et al., 2000). Heterogeneous reac-

[1]Ren, X., Brune, W. H., Oliger, A., Metcalf, A. R., Lesher, R. L., Simpas, J. B., Shirley, T., Schwab, J. J., Bai, C., Li, Y., Demerjian, K. L., and Roychowdhury, U.: OH and HO_2 during the PMTACS–NY Whiteface 2002 Campaign: Observations and Model Comparison, J. Geophys. Res., submitted, 2005b.

ACPD
5, 6041–6076, 2005

tions of HNO_3, SO_3, and N_2O_5 were included in the model. The assumption of steady-state certainly applies to OH, which had a lifetime shorter than 0.1 s and generally to HO_2, which has a lifetime less than a few 10 s of seconds.

The model was run with the FACSIMILE software (UES Software Inc). Model input was constrained to the ten-minute average values of O_3, NO, NO_2, CO, SO_2, categorized VOCs, water vapor, temperature, pressure, and photolysis frequencies, which were either measured if available or calculated with the NCAR TUV transfer model and scaled by measured solar UV radiation. The data coverage allowed model calculations only for the period between 14 April and 22 April. OH, HO_2, NO_3, organic peroxyl radicals (RO_2), and other intermediates were calculated. The uncertainty in this RACM model was estimated to be ±45% for OH and ±70% for HO_2, with 2σ confidence. These uncertainties are based on the combined uncertainties of the kinetic rate coefficients (Sander et al., 2003; Stockwell et al., 1997), the measured chemical concentrations, and the measured and calculated photolysis frequencies, as estimated with a Monte Carlo approach (as in Carslaw et al., 1999).

3. Results and discussion

MCMA 2003 was an excellent opportunity to study the atmospheric chemistry of a megacity that has improving air quality but still more air pollution than a typical US or European city. A goal of MCMA was to better understand the sources and chemical transformations of MCMA's air pollution. The suite of measurements assembled at the CENICA site enable calculations of atmospheric reactive constituents, particularly OH and HO_2, and of other pollution products. These calculations can then be compared to the observations.

The comparison of the observations at MCMA to those in US urban areas is also instructive. We compare our MCMA observations to our observations taken in New York City (NYC) in July 2001 (Ren et al., 2003a, b). New York City provides a good comparison because it is similar to MCMA in some ways, such as population, but

ACPD
5, 6041–6076, 2005

strikingly different in other ways, such as the ratio of VOCs to NO_x.

Ozone in MCMA 2003 was significantly greater than ozone in NYC in 2001 (Fig. 5a). The median MCMA O_3 peak of 100 ppbv was twice that of NYC. The maximum value occurred closer to local noon by about 2 h in MCMA than in NYC. Nighttime values were similar in the two locations, with minimum ozone at morning rush hour. In both studies, the observed ozone was less than typical due to atypical weather conditions.

Ozone production depends on both NO_x and VOCs. The speciated VOCs measured in MCMA 2003 have been compared to the typical US urban values (Lamb et al., 2004), which are not significantly different from the speciation in New York City, although total VOCs in MCMA were ~3 times larger than in the typical US city. However, NO_x was greater in Mexico City than in NYC only during morning rush hour (Fig. 5b), when, MCMA's median NO_x was 110 ppbv, almost twice NYC's NO_x. During the afternoon, both cities had about 20 ppbv of NO_x. Nighttime NO_x was typically 20–35 ppbv in both cities. Interestingly, the ratio of peak NO_x in the two cities – 2 – is similar to the ratio of peak O_3. The comparison of surface concentrations distorts the differences in NO_x and VOC emissions, since the midday mixed layer for MCMA was typically 4 km above the surface, while the mixed layer for NYC was typically 1 to 1.5 km. Thus, MCMA's emissions were substantially greater for both NO_x and VOCs.

3.1. OH reactivity measurements

In MCMA, the OH reactivity, k_{OH}, had a strong peak of ~120 s^{-1} during morning rush hour, 25 s^{-1} during midday, and ~35 s^{-1} at night (Fig. 6). It is also similar to the diurnal behavior of NO_x, which is consistent with a large transportation source of both OH reactivity and NO_x. This behavior contrasts with the OH reactivity in NYC, which was typically 20 s^{-1} the entire time, with a small increase during morning rush hour (Fig. 6). The MCMA morning peak is about 5 times what was found in NYC.

The comparison of the measured OH reactivity to the calculated OH reactivity is complicated by the timing of the two measurements during the study. Speciated VOCs

ACPD
5, 6041–6076, 2005

were measured just before and just after the period that OH reactivity was measured. A direct comparison is thus not possible. However, when the measured and calculated OH reactivity are plotted as a function of time of day, they are similar in absolute value and diurnal behavior (Fig. 6).

From calculations, 75±16 % of this reactivity is due to VOCs during daylight hours with the lowest values when NO_2 is greatest at 09:00 CST, while 84±7% is due to VOCs during night. Examining the OH reactivity due only to VOCs, the ratio of the OH reactivity per ppbC of VOCs was 0.056±0.017 s^{-1} $ppbC^{-1}$ in MCMA, but was ~3 times greater at 0.15±0.02 s^{-1} $ppbC^{-1}$ in NYC. This difference is consistent with the differences mainly in the alkane abundances between MCMA and typical US cities (Lamb et al., 2004). NYC in 2001 had approximately 1.5 times less VOCs than the typical US urban area.

3.2. OH and HO_2: measured and modeled values

OH was measured on 21 days in Mexico City from 5 April to 26 April 2003 (Fig. 7); HO_2 was measured on 18 days from 8 April to 26 April 2003 (Fig. 8). The NO addition to the HO_2 axis was deliberately delayed so that any potential interference that it might cause could be detected as a change in the OH measurement. No change was detected. OH was fairly consistent from day-to-day, with midday peak values of 0.25–0.4 pptv ((5–8)×10^6 cm^{-3}). The effects of clouds on OH production can be seen in the reduction in OH on several afternoons. Variability was greater for HO_2 than for OH. Peak HO_2 varied from 15 pptv (~3×10^8 cm^{-3}) to 60 pptv (~12×10^8 cm^{-3}).

The OH diurnal cycle becomes more distinct when OH is plotted as a function of time-of-day (Fig. 9a and c). The median OH peaks at 0.35 pptv (~7×10^6) cm^{-3} at local noon. The nighttime values ranged from 0.05 pptv (~1×10^6 cm^{-3}) to below the detection limit (0.01 pptv or 2×10^5 cm^{-3}) for 1-min measurements.

The observed OH in MCMA is similar to the observed OH in NYC, despite the large differences in OH reactivity, sunlight, and HO_x production rates between the two cities (Fig. 9a). The peak value in New York City is shifted 2 h past solar noon, but at 0.28 pptv

is only 20% lower than the average peak OH for MCMA.

The modeled OH shows similar behavior to the measured OH (Fig. 9c). The measured-to-modeled OH ratio is 1.07 during morning rush hour (05:00–09:00 CST), 0.77 during midday (10:00–14:00 CST), and 1.07 at night (20:00–04:00 CST). Daytime median modeled OH agrees with the daytime median OH measurements to well within the measurement uncertainty (±32%, 2σ confidence) and the model uncertainty. The linear fit of measured OH as a function of modeled OH has a slope of 0.65, and intercept of 0.026 pptv, and a correlation coefficient of 0.80. This slope is consistent with the tendency in the measured-to-modeled OH ratio, since the measured OH tends to be larger during the night and morning when OH is low while the modeled OH tends to be greater during midday, when the OH is greater. Relatively good agreement between median measured and modeled OH at night contrasts with poor agreement exceeding a factor of 5 in some other urban environments (Martinez et al., 2003; Ren et al., 2003b).

The HO_2 peak is narrower than the OH peak and is shifted one hour later. HO_2 persisted at ~5 pptv (0.5 to 20 pptv) during the night. HO_2 has a diurnal profile that peaked at ~40 pptv at 13:00, and decreased to less than 0.5 pptv at sunrise, when HO_x production was just beginning to increase but when copious rush-hour NO effectively scavenged HO_2.

The HO_2 in MCMA was generally ten times larger than the HO_2 was in NYC (Fig. 9b). This large difference results from the large difference in the HO_x sources, although the MCMA photolysis frequencies were only about twice those in NYC. The big difference is the greater amount of HCHO in MCMA. It peaks at ~20 ppbv in the morning (R. Volkamer, private communication, 2005), represents about 40% of the HO_x source, and is about 15 times larger in MCMA than in NYC during midday. Ozone, which is twice as large in MCMA as in NYC, also contributes to the difference in HO_x. The HO_x sink, which is predominantly the reaction $OH+NO_2+M \rightarrow HNO_3+M$, is comparable in the two cities except during morning rush hour, when it is twice as large in MCMA. The difference in OH reactivity translates directly into the difference in HO_x, which in turn

ACPD
5, 6041–6076, 2005

determines the ozone production rates.

The model simulates the median measured HO_2 to well within the measurement and modeling uncertainties (Fig. 9d). The midday measured-to-modeled ratio is 0.79; the nighttime ratio is 1.25. During morning rush hour, the observed-to-modeled ratio is 1.17. The linear fit of measured HO_2 as a function of modeled HO_2 has a slope of 0.70, and intercept of 3.4 pptv, and a correlation coefficient of 0.64. The model appears to produce too much HO_x during the daytime.

These MCMA HO_x measurements are a good example of the buffering effects of the OH production and loss processes. Over the course of the study, HO_2 peak values varied greatly from day-to-day, indicating dramatic changes in HO_x sources, but OH peak values remained relatively unchanged, as can be seen by comparing Figs. 7 and 8 and by comparing the MCMA and NYC median HO_x values in Fig. 9. That HO_2 is much more sensitive to HO_x sources and sinks than OH suggests that HO_2 must be measured along with OH to really test and understand the radical chemistry.

For MCMA 2003 midday HO_2/OH was typically 120, with low values of 10–15 during morning rush hour and high values of 200 at night (Fig. 10). This behavior is quite different from New York City, where the ratio was typically ~15 at all times (Ren et al., 2003a). The difference in the midday HO_2/OH ratio between MCMA and NYC is due to differences in NO, which was typically less than 1 ppbv in MCMA but 5 ppbv or higher in NYC, and the OH reactivity, which in MCMA was typically 1.5 times that in NYC. When HO_x cycling is faster than HO_x production and loss, the HO_2/OH ratio is approximately given by the equation:

$$\frac{[HO_2]}{[OH]} \approx \frac{k_{OH}[OH]}{k_{NO+HO_2}[NO]} \quad (7)$$

Increasing the numerator in Eq. (7) by 1.5 and decreasing the denominator by ~5 provides the difference in the MCMA and NYC HO_2/OH ratios.

The measured HO_2/OH ratios display the same dependence on NO as the modeled ratio (Fig. 10) for NO between 1 and 100 ppbv. Both the measured and modeled ratios

ACPD
5, 6041–6076, 2005

vary approximately as the $\frac{1}{2}$ power of NO, whereas an NO power dependence of 1 to 2 is expected. This less-than-theory power dependence comes from the co-emission with NO of atmospheric constituents that react with OH, thus increasing HO_2. While such good agreement between the measured and modeled ratio is expected, this behavior is not observed in some other urban areas. Typically, the measured HO_2/OH has had a much shallower slope with respect to NO than the modeled ratio does (Ren et al., 2003; Martinez et al., 2003; Emmerson, 2005).

3.3. OH production and loss

MCMA's OH reactivity of $20\,s^{-1}$ during most of the day and $120\,s^{-1}$ at morning rush hour implies OH lifetimes of 50 ms to 8 ms. This lifetime is much shorter than the time scales for other processes, including mixing of emissions, changes in photolysis, and other chemistry. As a result, OH should always be in steady-state. The OH production should equal the OH loss:

$$P(OH)=2J_{O3}f[O_3][H_2O] + J_{HONO}[HONO] + k_{NO+HO2}[NO][HO_2] + k_{O3+VOC}[O_3][VOC] + \text{other smaller terms} = k_{OH}[OH] = L(OH) \quad (8)$$

f is the fraction of $O(^1D)$ that is produced from O_3 photolysis and reacts with H_2O to produce OH. The OH loss is determined simply from the product of [OH] and the OH reactivity, both of which are measured. Over 80% of the OH production is controlled by $[HO_2]$ and [NO], both of which are measured. The first three OH production terms were calculated from measurements; the fourth term, OH production from O_3 and alkenes, was taken from model results and was less than 5% of the total.

P(OH) and L(OH) are in balance to within the combined 2σ uncertainties of the OH production and loss terms (Fig. 11). The difference L(OH) – P(OH) should be zero for the entire day, but it is actually slightly negative during morning rush hour (05:00-09:00 CST), implying greater-than-expected production. Smaller L(OH) – P(OH) differences at morning rush hour were observed in Nashville (Martinez et al., 2003) and in New York City (Ren et al., 2003a).

ACPD
5, 6041–6076, 2005

These differences at morning rush hour are not beyond the measurement uncertainties, and yet they are persistent from study to study. For MCMA between 07:00 and 08:00 CST, OH production is double the OH loss. Previous attempts to explain these differences with instrumental artifacts for HO_2 have failed (Ren et al., 2004); however, it is possible that our laboratory tests of the correction algorithm for $HO_2+NO \rightarrow OH+NO_2$ do not apply to MCMA air, with its more complex composition. This explanation, however, seems unlikely.

If the measurements are correct, then the imbalance in the OH production and loss at morning rush hour indicates problems with known urban photochemistry. We are left with the conclusion that some aspect of the HO_x-NO_x photochemistry may need re-examination. One solution would be that some products of the reaction HO_2+NO are not $OH+NO_2$. Instead, this imbalance provides evidence that some of the HO_2+NO reaction results either in HO_x removal or couples with another reaction that rapidly cycles back to HO_2 without going through OH. The uncertainty in the MCMA measurements does not allow us to distinguish between HO_x removal or rapid cycling. A study of the imbalance in the NO_x photostationary state led Volz-Thomas et al. (2003) to a similar and possibly related conclusion: an unknown process is converting NO to NO_2 without resulting in ozone production.

3.4. Instantaneous O_3 production

The net instantaneous O_3 production is in some ways a better indicator of the connection between ozone precursors and ozone than is the ozone mixing ratio itself (Kleinman et al., 2000). Instantaneous ozone production is not subject to the uncertainties in physical processes like horizontal advection, planetary boundary layer height changes, entrainment of free-tropospheric air, and dry deposition. On the other hand, because it does not take these physical processes into account, it is a poor indicator of the actual ozone mixing ratios that will occur. Never-the-less, it does provide insight into the chemical processes that create ozone at the CENICA site.

The net instantaneous photochemical O_3 production can be calculated by the equa-

tion:

$$P(O_3)=k_{HO2+NO}[NO][HO_2] + \Sigma k_{RO2i+NO}[NO][RO_{2i}]-k_{OH+NO2+M}[M][NO_2][OH]-P(RONO_2) \quad (9)$$

For urban environments like MCMA, including the NO_2 lost to HNO_3 or organic nitrate ($RONO_2$) formation can offset ~10% of the ozone production and must be included. If $P(O_3)$ is calculated only from the measured quantities HO_2, NO, OH, and NO_2, then only the first and the third terms are retained. This reaction, of course, assumes that all of HO_2+NO forms OH+NO_2 and that NO_2 is photolyzed to produce ozone.

For the period between 14 April and 22 April when the measurement suite was complete enough for model runs, $P(O_3)$ calculated from measured HO_2 peaked at 48 ppbv hr^{-1} while $P(O_3)$ calculated from modeled HO_2 peaked at 86 ppbv hr^{-1} (Fig. 12). Both peaks are broad and achieve maximum values near 10:00 CST. Peak values on some days were greater than 100 ppbv hr^{-1}. The greater modeled $P(O_3)$ in late morning is due to the greater modeled HO_2 then.

The NO_x peak at morning rush hour is mainly due to fresh NO emissions (Fig. 5). Beginning at about 05:00 CST, O_3 was drawn down by the reaction with NO to form NO_2, but the sum of NO_2+O_3 remained relatively constant. As $P(O_3)$ began to increase at 06:00 CST, NO_2+O_3 began to increase, but more than 90% of the produced O_3 was partitioned into NO_2 by reaction with NO. O_3 did not begin to really rise until about 07:30 CST, when NO had fallen to half its peak value and $J(NO_2)$ had climbed to 16% of its peak value. Thus, the sum of NO_2+O_3 rose along with $P(O_3)$, while the O_3 rise appears to have been delayed by about 1.5 h (Fig. 12).

In New York City, the median mid-morning $P(O_3)$ from HO_2 was 12 ppbv hr^{-1}, peaking at 11 EDT. On a few days, $P(O_3)$ from HO_2 reached as high as 50 ppbv hr^{-1}, but on many days, its peak value was less than 10 ppbv hr^{-1}. This ozone production rate from HO_2 is about five times smaller than that observed in MCMA. The differences in the measured HO_2 in MCMA and NYC is the difference in $P(O_3)$.

$P(O_3)$ is expected to increase until NO reaches a few ppbv, after which $P(O_3)$ decreases as HO_2 begins to decrease greater than linearly with NO. In some environ-

ments, $P(O_3)$ did not have the expected decrease as NO exceeded a few ppbv (Martinez et al., 2003; Ren et al., 2003a, 2005a). This unexpected behavior can be directly attributed to the less-than-expected decrease in HO_2 or HO_2+RO_2 at greater NO. In MCMA 2003, the behavior of HO_2 as a function of NO is not dramatically different from the model (see Fig. 12). If the measurements and models are segregated into data for which HO_x production exceeded 2×10^7 molecules cm^{-3} s^{-1}, which are typically mid-day values, and for HO_x production for 10^6 – 10^7 molecules cm^{-3} s^{-1}, which is typical of morning and evening rush hour, the $P(O_3)$ calculated from measured and modeled HO_2 show similar behavior as a function of NO (Fig. 13). The data are sparse, but $P(O_3)$ appears to peak when NO is 20 to 30 ppbv.

It is not clear why $P(O_3)$ calculated from measured HO_2 appears to behave as expected for MCMA 2003 while it did not for other urban areas. New York City in wintertime is an extreme example of unexpected behavior (Ren et al., 2005a). It has been speculated that the greater-than-expected HO_2 at greater NO is due to unknown HO_x-NO_x chemistry. Since the greatest difference between NYC and MCMA is the VOC levels, it may be that the rapid cycling of HO_x through VOC chemistry reduces the impact of the unknown HO_x-NO_x chemistry on HO_2.

The cumulative daily surface ozone production from HO_2 at the CENICA site was calculated to be 319 ppbv by measurement and 335 ppbv by model. The model suggests that the total ozone production from HO_2 and RO_2 was 629 ppbv, since modeled RO_2 was typically 1.5 times modeled HO_2. These cumulative values are for the CENICA site only. To relate ozone production to observed ozone requires the knowledge of the temporal and spatial variations of $P(O_3)$ and O_3 throughout the MCMA.

4. Summary and conclusions

The MCMA 2003 study stretched the envelope of the pollution levels for which such a complete set of atmospheric measurements that included OH and HO_2 have been obtained. We summarize several conclusions from this study.

First, even in an environment with such high loadings of NO_x and VOCs, steady-state photochemical models were generally able to simulate the measured OH and HO_2. The model tends to produce too little OH and HO_2 during night and morning rush hour and too much during midday. We are investigating to see if these differences are due to errors in the HO_x sources or the HO_x in the model. The agreement between the measured and modeled HO_x is as good as or better than that obtained in other urban environments (George et al., 1999; Martinez et al., 2003; Ren et al., 2003b; Heard et al., 2004).

Second, a surprising result is the good agreement between the measured and modeled HO_2/OH ratio as a function of NO. This agreement is better than we have seen in any other environment where NO exceeded a few ppbv. The difference between these other urban areas and MCMA is not particularly the NO_x abundance, which is similar to that in New York City, but instead is the large amounts of VOCs, which result in high OH reactivities.

Third, while the OH sources and sinks are both substantially increased over those in US cities, the resulting OH is similar to that observed in US cities. Not so for HO_2, which was greater in MCMA than in US cities and thus directly responsible for the differences seen in the ozone levels between MCMA and US cities.

Fourth, the OH reactivity was higher than we have observed in any other environment, reaching more than $120\,s^{-1}$ in morning rush hour. Our correction scheme for $HO_2+NO \rightarrow OH+NO_2$ allows OH reactivity measurements in much more polluted environments than before. While the overlap between measured OH reactivity and speciated VOCs was poor, the diurnal patterns and values are qualitatively similar. This observation is consistent with our observations in New York City and Houston, Texas, unlike our measurements in Nashville (Kovacs et al., 2003) and other measurements in Tokyo (Sadanaga et al., 2004), both of which were 30% greater than calculated OH reactivity.

Fifth, the balance between OH production and OH loss is generally consistent with the expected OH steady state balance. A possible exception is during morning rush

ACPD
5, 6041–6076, 2005

hour when OH production exceeds OH loss by as much as a factor of two. While the differences are not statistically significant, they do bear watching because they suggest errors in HO_x-NO_x photochemistry.

Sixth, the apparent good agreement between the net instantaneous ozone production calculated from measured HO_2 and from modeled HO_2 stands in contrast to previous urban studies. Examining the differences between the atmospheric compositions in these different environments may illuminate the cause of the unexpected results in the other studies.

Finally, the combination of high OH reactivity, abundant sunlight, and NO_x at morning rush hour jump starts ozone production, which from HO_2 alone reached ~50 ppbv hr^{-1} by mid-morning. Similar results are found by R. Volkamer (private communication, 2005). Had the meteorological conditions not produced afternoon clouds, occasional rain, and below normal temperatures, midday ozone levels would have been greater.

Acknowledgements. We thank the entire MCMA team for the support they provided us during the MCMA 2003 campaign and for the stimulating discussions at the science workshop. We also thank our colleagues for the use of their data for our model calculations. This work was supported by NSF Atmospheric Chemistry grants (ATM-0209972 and ATM-308748) and the Comisión Ambiental Metropolitana of Mexico. R. Volkamer acknowledges the Henry and Camille Dreyfus Foundation for a Dreyfus postdoctoral fellowship.

References

Carslaw, N., Jacoba, P. J., and Pilling, M. J.: Modeling OH, HO_2, and RO_2 radicals in the marine boundary layer, 2. Mechanism reduction and uncertainty analysis, J. Geophys. Res., 104, 30 257–30 273, 1999.

Di Carlo, P., Brune, W. H., Martinez, M., Harder, H., Lesher, R., Ren, X., Thornberry, T., Carroll, M. A., Young, V., Shepson, P. B., Riemer, D., Apel, E., and Campbell, C.: Missing OH reactivity in a forest: Evidence for unknown reactive biogenic VOCs, Science, 304, 722–725, 2004.

Emmerson, K. M., Carslaw, N., Carpenter, L. J., Heard, D. E., Lee, J. D., and Pilling, M. J.: Urban Atmospheric Chemistry during the PUMA Campaign, 1: Comparison of Modelled OH and HO_2 Concentrations with Measurements, J. Atmos. Chem., in press, 2005.

Faloona, I. C., Tan, D., Lesher, R. L., Hazen, N. L., Frame, C. L., Simpas, J. B., Harder, H., Martinez, M., Di Carlo, P., Ren, X., and Brune, W. H.: A laser induced fluorescence instrument for detecting tropospheric OH and HO_2: Characteristics and calibration, J. Atmos. Chem., 47, 139–167, 2004.

Fenske, J. D., Hasson, A. S., Paulson, S. E., Kuwata, K. T., Ho, A., and Houk, K. N.: The pressure dependence of the OH radical yield from ozone-alkene reactions, J. Phys. Chem. A, 104, 7821–7833, 2000.

George, L. A., Hard, T. M., and O'Brien, R. J.: Measurement of free radicals OH and HO_2 in Los Angeles Smog, J. Geophys. Res., 104, 11 643–11 655, 1999.

Hard, T. M., O'Brien, R. J., Chan, C. Y., and Mehrabzadeh, A. A.: Tropospheric free radical determination by FAGE, Environ. Sci. Technol., 18, 768–777, 1984.

Heard, D. E., Carpenter, L. J., Creasey, D. J., Hopkins, J. R., Lee, J. D., Lewis, A. C., Pilling, M. J., Seakins, P. W., Carslaw, N., and Emmerson, K. M.: High levels of the hydroxyl radical in the winter urban troposphere, Geophys. Res. Lett., 31, doi:10.1029/2004GL020544, 2004.

Kleinman, L. I.: Ozone process insights from field experiments – part II: Observation-based analysis for ozone production, Atmos. Environ., 34, 2023–2033, 2000.

Kovacs, T. A. and Brune, W. H.: Total OH loss rate measurement, J. Atmos. Chem., 39, 105–122, 2001.

Kovacs, T. A., Brune, W. H., Harder, H., Martinez, M., Simpas, J. B., Frost, G. J., Williams, E., Jobson, T., Stroud, C., Young, V., Fried, A., and Wert, B.: Direct measurements of urban OH reactivity during Nashville SOS in summer 1999, J. Environ. Monit., 5, 68–74, doi:10.1039/b204339d, 2003.

Lamb, B., Velasco, E., Allwine, E., Westberg, H., Herndon, S., Knighton, B., Grimsrud, E., Jobson, T., Alexander, M., and Prezeller, P.: Ambient VOC measurements in Mexico City, American Meteorological Society Fifth Conference on Urban Environment, Vancouver, BC, Canada, August 23–26, 2004.

Martinez, M., Harder, H., Kovacs, T. A., Simpas, J. B., Bassis, J., Lesher, R., Brune, W. H., Frost, G. J., Williams, E. J., Stroud, C. A., Jobson, B. T., Roberts, J. M., Hall, S. R., Shetter, R. E., Wert, B., Fried, A., Alicke, B., Stutz, J., Young, V. L., White, A. B., and Zamora, R. J.: OH and HO_2 concentrations, sources, and loss rates during the South-

ern Oxidants Study in Nashville, Tennessee, summer 1999, J. Geophys. Res., 108, 4617, doi:10.1029/2003JD003551, 2003.
Martinez, M., Harder, H., Brune, W., Di Carlo, P., Williams, E., Hereid, D., Jobson, T., Kuster, W., Roberts, J., Trainer, M., Fehsenfeld, F. C., Hall, S., Shetter, R., Apel, E., Riemer, D., and Geyer, A.: The behavior of the hydroxyl and hydroperoxyl radicals during TexAQS2000, Abstract A12D-0174, AGU Fall Meeting, EOS Transactions, San Francisco, California, 2002.
Molina, L. T. and Molina, M. J. (Eds.): Air Quality in the Mexico Megacity: An integrated assessment, Kluwer Academic Publishers, Boston, pp. 105–136, 2002.
Paulson, S. E., Chung, M. Y., and Hasson, A. S.: OH radical formation from the gas-phase reaction of ozone with terminal alkenes and the relationship between structure and mechanism, J. Phys. Chem. A, 103, 8125–8138, 1999.
Ren, X., Harder, H., Martinez, M., Lesher, R. L., Oliger, A., Shirley, T., Adams, J., Simpas, J. B., and Brune, W. H.: HO_x concentrations and OH reactivity observations during the PMTACS-NY 2001 campaign in New York City, Atmos. Environ., 37, 3627–3637, 2003a.
Ren, X., Harder, H., Martinez, M., Lesher, R. L., Oliger, A., Simpas, J. B., Brune, W. H., Schwab, J. J., Demerjian, K. L., He, Y., Zhou, X., and Gao, H.: OH and HO_2 chemistry in the urban atmosphere of New York City, Atmos. Environ., 37, 3639–3651, 2003b.
Ren, X., Harder, H., Martinez, M., Faloona, I., Tan, D., Lesher, R. L., Di Carlo, P., Simpas, J. B., and Brune, W. H.: Interference testing for atmospheric HO_x measurements by laser-induced fluorescence, J. Atmos. Chem., 47, 169–190, 2004.
Ren, X., Shirley, T., Metcalf, A. R., Lesher, R. L., Brune, W. H., Cantrell, C. A., and Edwards, G. D.: Hydroxyl and Peroxy Radical Chemistry in a Rural Area of Central Pennsylvania: Observations and Model Comparisons, J. Atmos. Chem., in press, 2005a.
Rickard, A. R., Johnson, D., McGill, C. D., and Marston, G.: OH yields in the gas-phase reactions of ozone with alkenes, J. Phys. Chem. A, 103, 7656–7664, 1999.
Sadanaga, Y., Yoshino, A., Kato, S., Yoshioka, A., Watanabe, K., Miyakawa, Y., Hayashi, I., Ichikawa, M., Matsumoto, J., Nishiyama, A., Akiyama, N., Kanaya, Y., and Kajii, Y.: The importance of NO_2 and volatile organic compounds in the urban air from the viewpoint of the OH reactivity, Geophys. Res. Lett., 31, L08102, doi:10.1029/2004GL019661, 2004.
Sander, S. P., Friedl, R. R., Golden, D. M., Kurylo, M. J., Huie, R. E., Orkin, V. L., Moortgat, G. K., Ravishankara, A. R., Kolb, C. E., Molina, M. J., and Finlayson-Pitts, B. J.: Chemical kinetics and photochemical data for use in stratospheric modeling, Evaluation Number 14, JPL Publication 02–25, NASA Jet Propulsion Laboratory, Pasadena, CA, 2003.

Stockwell, W. R., Kirchner, F., and Kuhn, M.: A new mechanism for regional atmospheric chemistry modeling, J. Geophys. Res., 102, 25 847–25 879, 1997.

Tanner, D. J. and Eisele, F. L.: Present OH measurement limits and associated uncertainties, J. Geophys. Res., 100, 2883–2892, 1995.

Volz-Thomas, A., Geiss, H., Hofzumahaus, A., and Becker, K.-H.: Introduction to Special Section: Photochemistry Experiment in BERLIOZ, J. Geophys. Res., 108, 8252, doi:10.1029/2001JD002029, 2003.

Volz-Thomas, A., Pätz, H.-W., Houben, N., Konrad, S., Mihelcic, D., Klüpfel, T., and Perner, D.: Inorganic trace gases and peroxy radicals during BERLIOZ at Pabstthum: An investigation of the photostationary state of NO_x and O_3, J. Geophys. Res., 108(D4), 8248, doi:10.1029/2001JD001255, 2003.

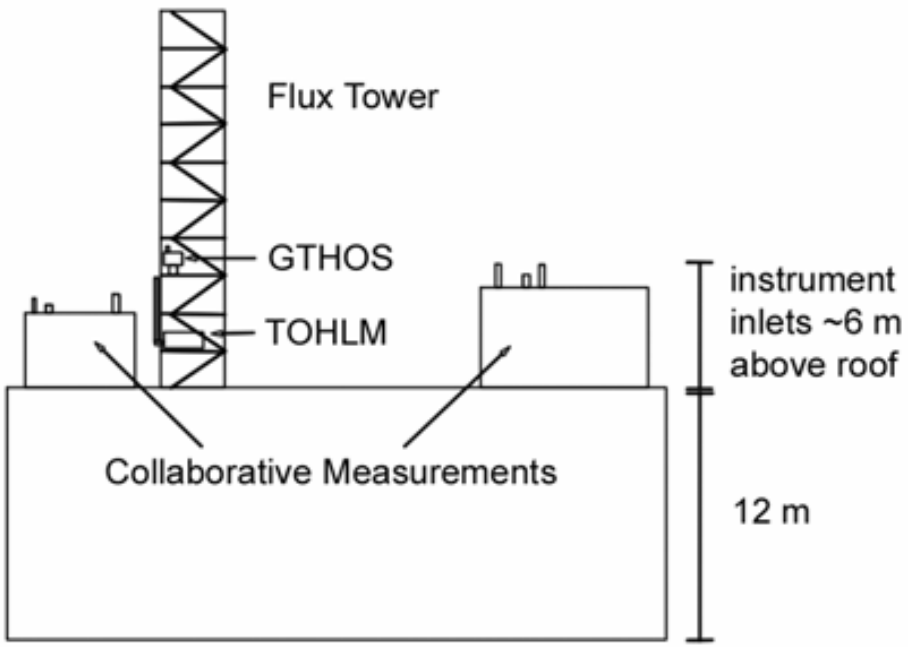

Fig. 1. Schematic of the instruments on the CENICA building roof. Both the Penn State instruments (GTHOS and TOHLM) were on the flux tower with their inlets within 1 m of one another. Collaborative measurements were also taken on the rooftop by other research groups.

ACPD
5, 6041–6076, 2005

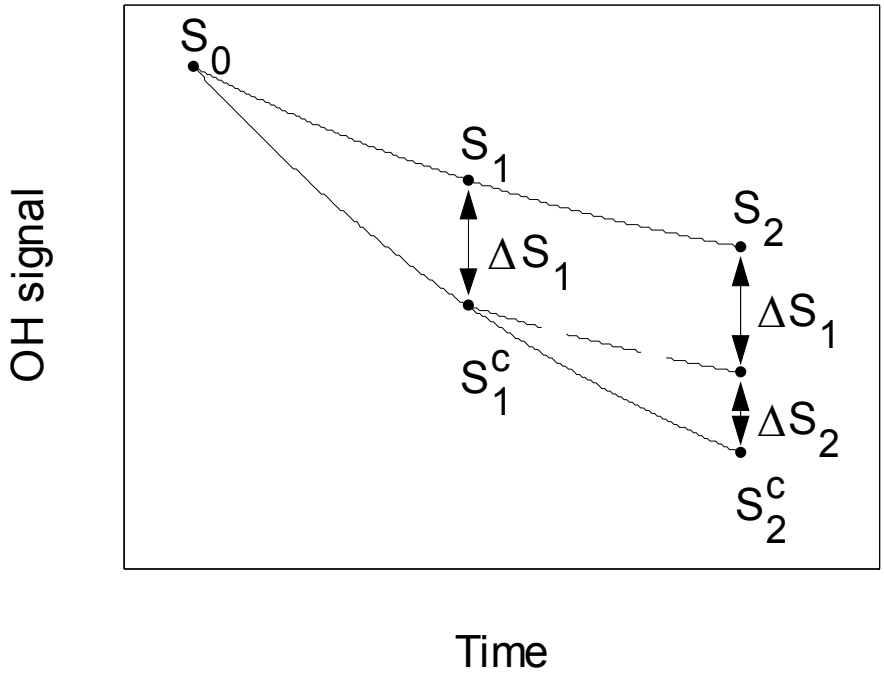

Fig. 2. An example of correcting an OH decay for NO interference. The top curve represents the OH decay with NO interference; the bottom curve is the corrected decay.

ACPD
5, 6041–6076, 2005

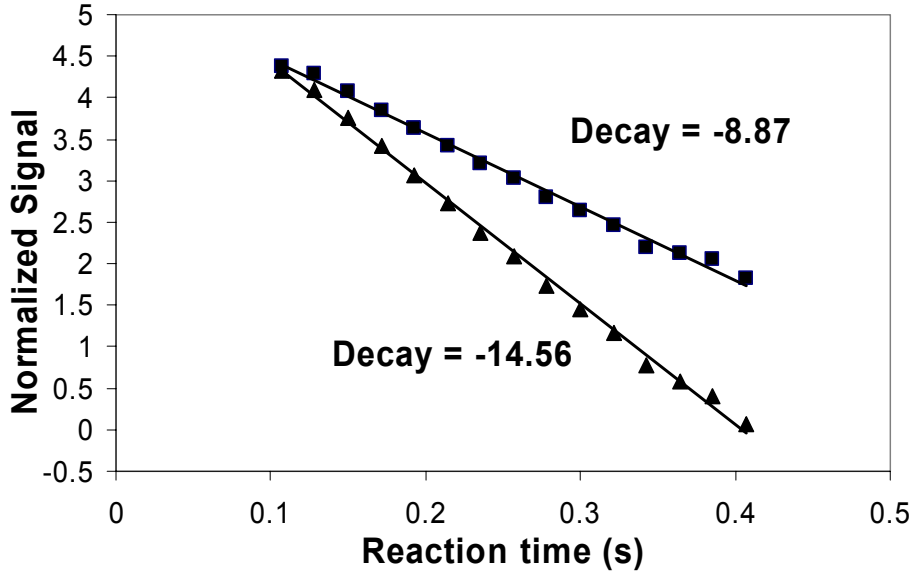

Fig. 3. Laboratory test of the NO correction technique with an average NO concentration of 76.5 ppbv. The top curve represents the original OH decay (squares) with a calculated decay rate of 8.9 s^{-1}; the bottom curve is the corrected OH decay (triangles) with a calculated decay rate of 14.6 s^{-1}. The theoretical decay rate is 14.9 s^{-1}.

ACPD
5, 6041–6076, 2005

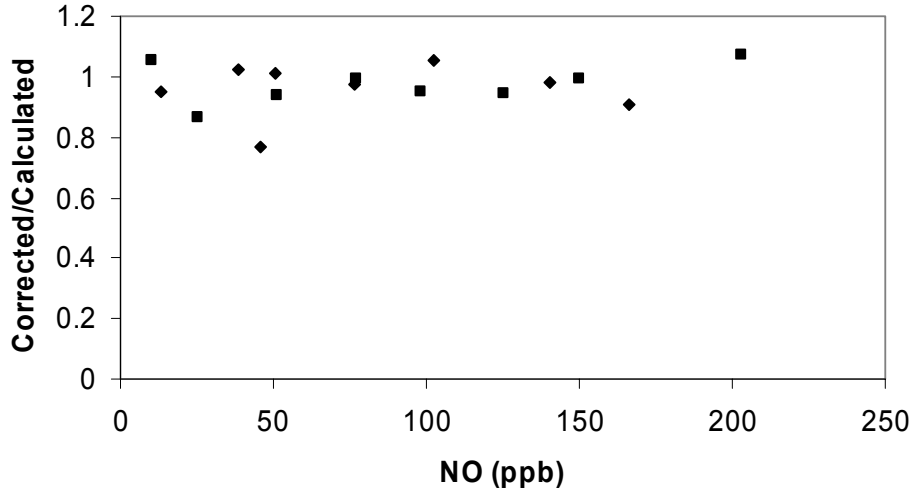

Fig. 4. The ratio of corrected OH decays to the theoretical calculated decays for a wide range of NO values. Decays with just NO (diamonds) and with NO and CO (squares) are both corrected to the expected value with this technique.

ACPD
5, 6041–6076, 2005

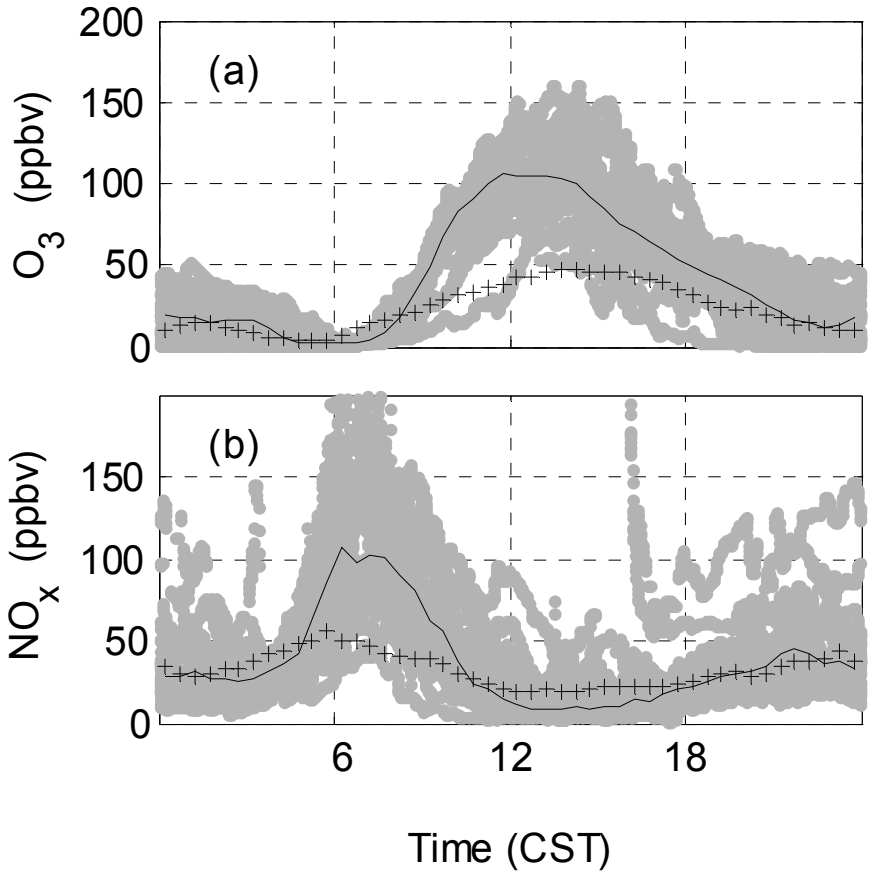

Fig. 5. Diurnal variation of pollutants. **(a)** Median ozone in MCMA 2003 (solid line) and NYC 2001 (plusses). **(b)** Median NO_x in MCMA 2003 (solid line) and NYC 2001 (plusses). Gray dots are individual MCMA measurements.

ACPD
5, 6041–6076, 2005

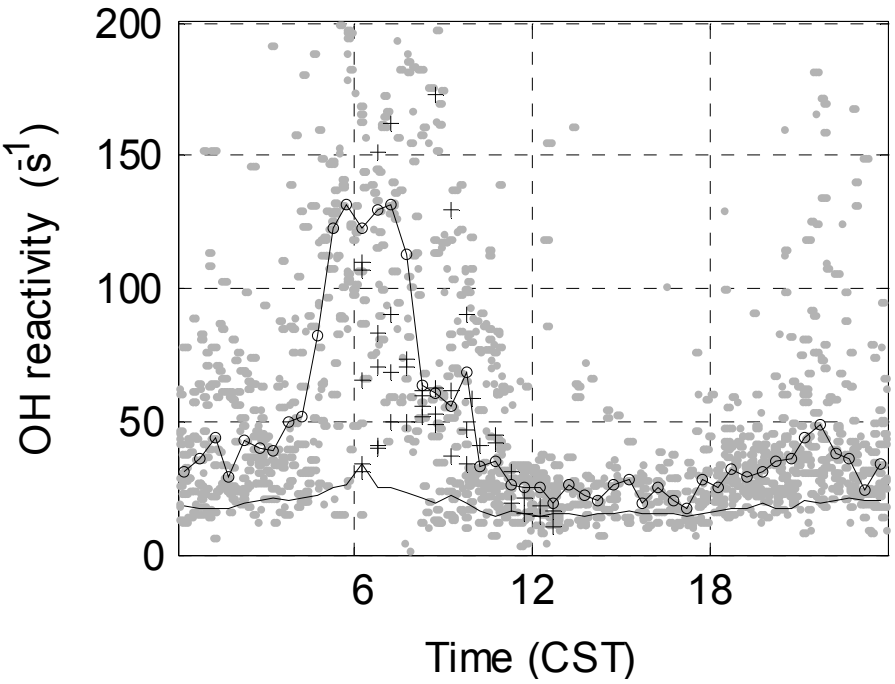

Fig. 6. Diurnal variation of median measured OH reactivity in MCMA 2003 (connected circles) and NYC 2001 (solid line). Gray points are individual MCMA measurements. Plusses are the composite median profile of OH reactivity calculated from the measured inorganic and VOC species. Scatter in the calculated OH reactivity is similar to the scatter in the measured OH reactivity (gray dots).

ACPD
5, 6041–6076, 2005

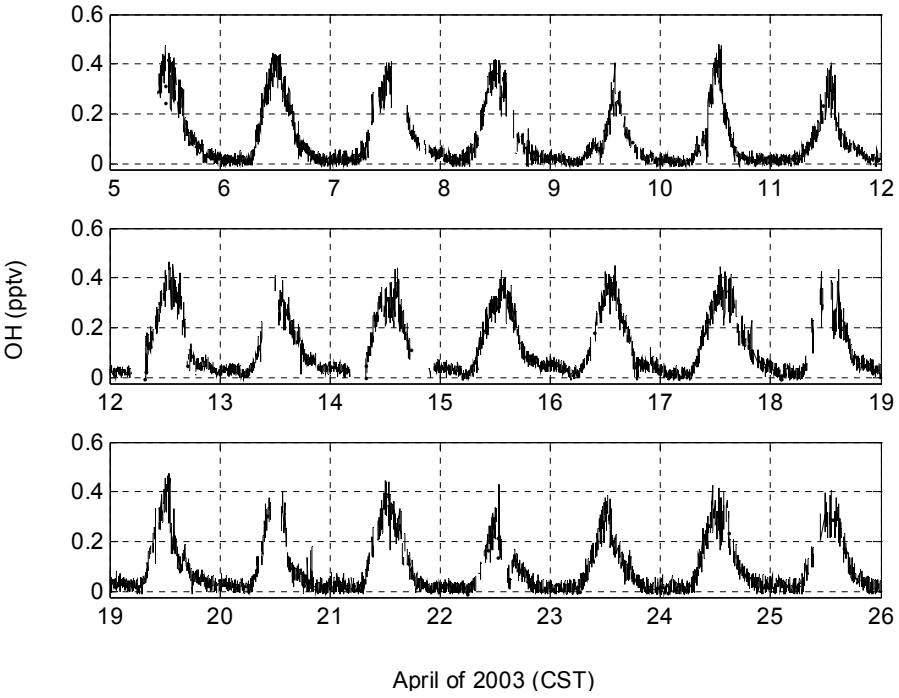

Fig. 7. Time series in CST of all the 1-min averaged OH data during the MCMA-2003 study.

ACPD
5, 6041–6076, 2005

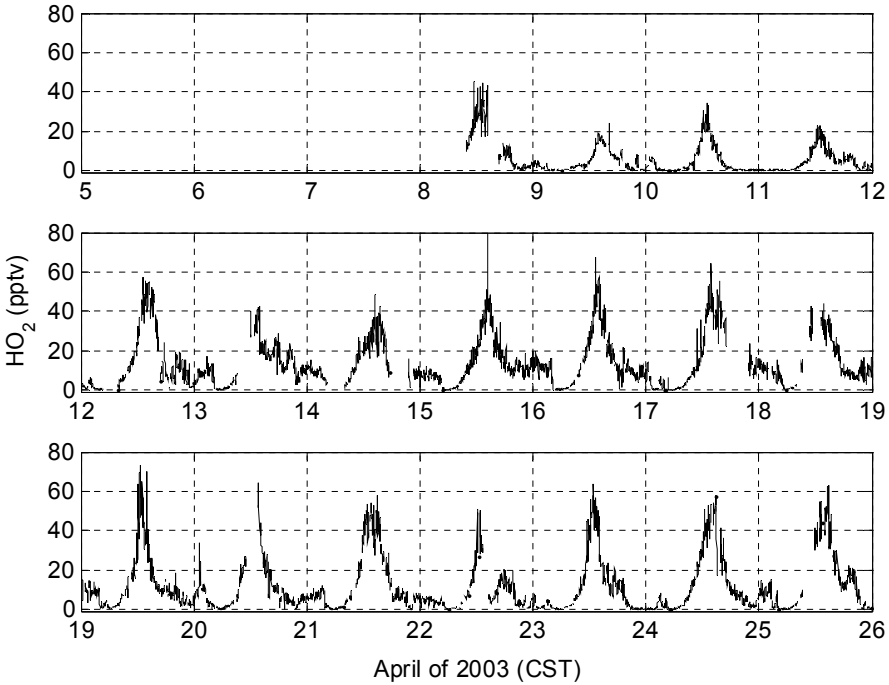

Fig. 8. Time series in CST of all the one-minute averaged HO_2 data during the MCMA-2003 study.

ACPD
5, 6041–6076, 2005

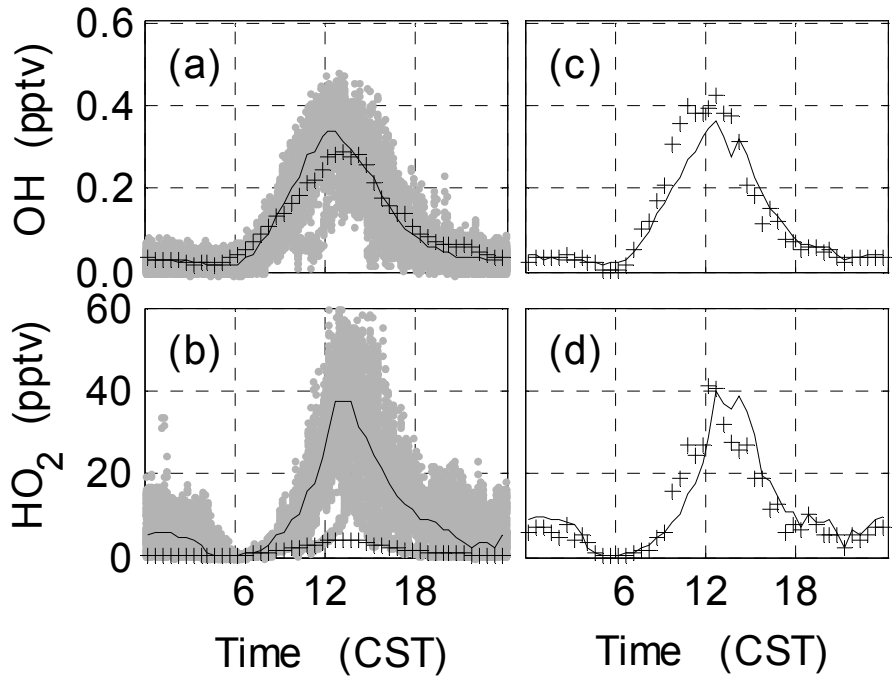

Fig. 9. Diurnal variation of OH and HO_2 for MCMA between 11 April and 21 April. **(a)** Measured OH in MCMA (solid line) and in NYC (plusses); **(b)** measured HO_2 in MCMA (solid line) and NYC (plusses); **(c)** measured OH (solid line) and modeled OH (plusses) in MCMA; **(d)** measured HO_2 (solid line) and modeled HO_2 (plusses) in MCMA. Gray dots are individual MCMA measurements.

ACPD
5, 6041–6076, 2005

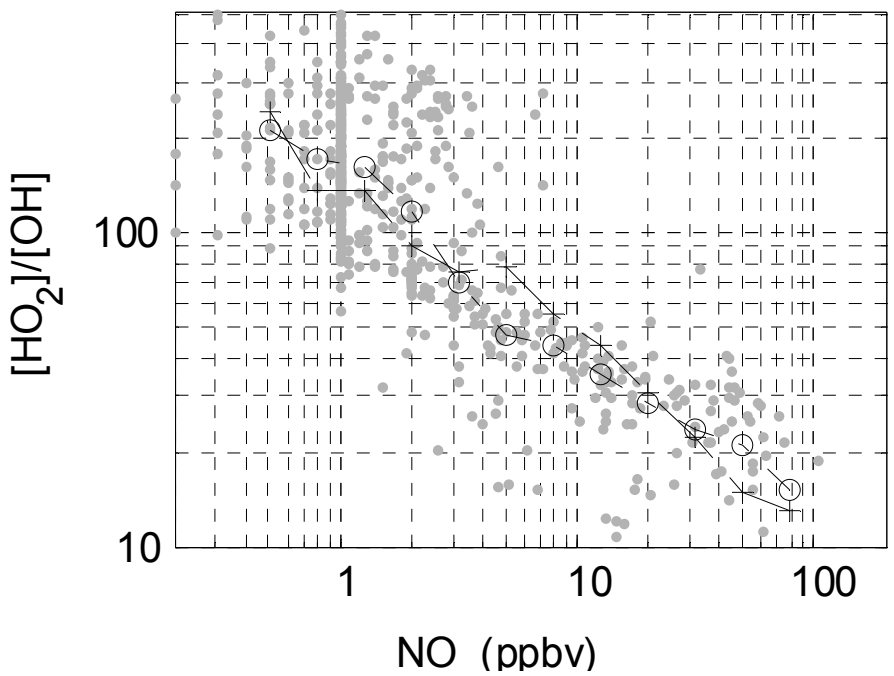

Fig. 10. Dependence of the measured (o) and modeled (+) $[HO_2]/[OH]$ ratio with NO. Gray dots are individual 10-min measurements. Lines are added to aid comparison.

ACPD
5, 6041–6076, 2005

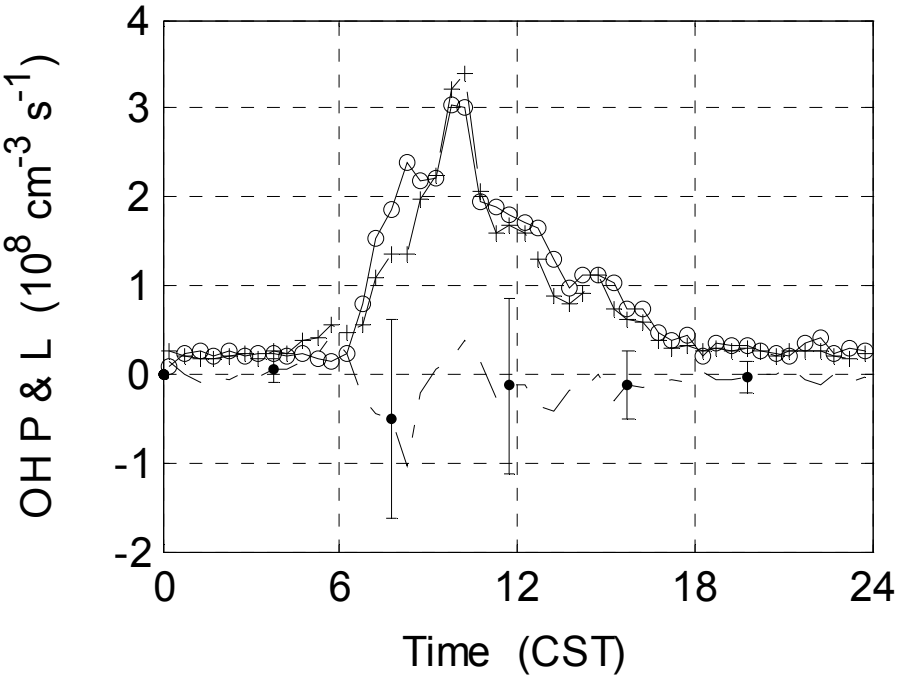

Fig. 11. Diurnal variation of the median OH production (circles) and median loss (plusses), and median loss – production (dot-dash line) for MCMA. Error bars are 2-σ absolute uncertainty on OH loss – OH production.

ACPD
5, 6041–6076, 2005

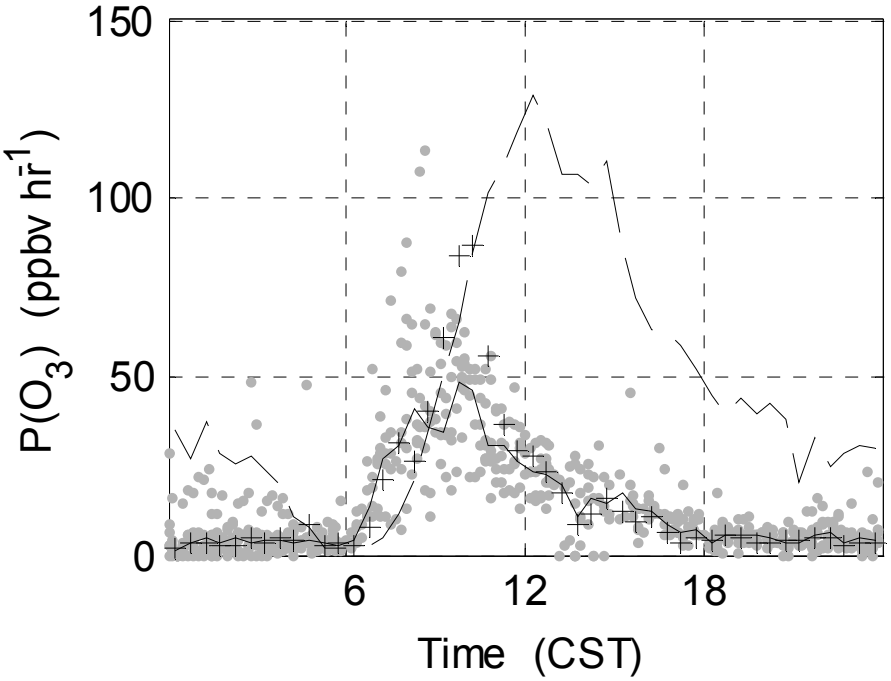

Fig. 12. Diurnal average of instantaneous photochemical ozone production ($P(O_3)$). 30-min median $P(O_3)$ from measured HO_2 (solid line) is compared to 30-min median $P(O_3)$ from modeled HO_2 (plusses). Median observed ozone is the dashed line. Gray dots are individual 30-min median $P(O_3)$ from measured HO_2.

ACPD
5, 6041–6076, 2005

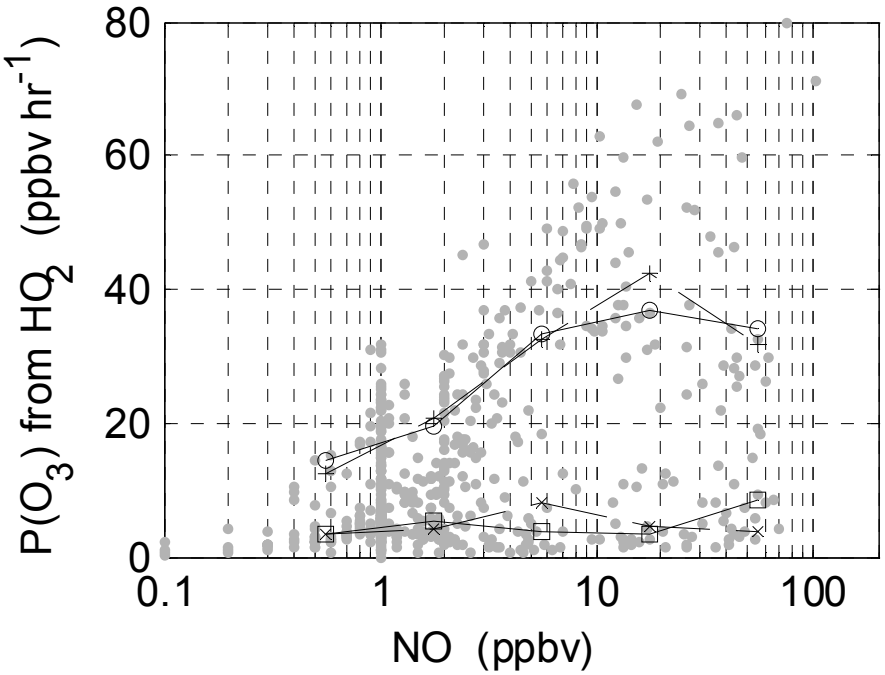

Fig. 13. $P(O_3)$ from HO_2 as a function of NO. Median $P(O_3)$ is plotted for HO_x production $>2\times10^7$ molecules cm^{-3} s^{-1} as calculated from measured (circles, solid line) and modeled (plusses, dashed line) HO_2 and for HO_x production of 10^6–10^7 molecules cm^{-3} s^{-1} for measured (squares, solid line) and modeled (x's, dashed line) HO_2. Gray dots are individual $P(O_3)$ from measured HO_2.

ACPD
5, 6041–6076, 2005